ITU-R
Radiocommunication Sector of ITU

Recommendation ITU-R P.619-3
(12/2017)

Propagation data required for the evaluation of interference between stations in space and those on the surface of the Earth

P Series

Radiowave propagation

International Telecommunication Union

Foreword

The role of the Radiocommunication Sector is to ensure the rational, equitable, efficient and economical use of the radio-frequency spectrum by all radiocommunication services, including satellite services, and carry out studies without limit of frequency range on the basis of which Recommendations are adopted.

The regulatory and policy functions of the Radiocommunication Sector are performed by World and Regional Radiocommunication Conferences and Radiocommunication Assemblies supported by Study Groups.

Policy on Intellectual Property Right (IPR)

ITU-R policy on IPR is described in the Common Patent Policy for ITU-T/ITU-R/ISO/IEC referenced in Annex 1 of Resolution ITU-R 1. Forms to be used for the submission of patent statements and licensing declarations by patent holders are available from http://www.itu.int/ITU-R/go/patents/en where the Guidelines for Implementation of the Common Patent Policy for ITU-T/ITU-R/ISO/IEC and the ITU-R patent information database can also be found.

<div style="border:1px solid">

Series of ITU-R Recommendations

(Also available online at http://www.itu.int/publ/R-REC/en)

Series	Title
BO	Satellite delivery
BR	Recording for production, archival and play-out; film for television
BS	Broadcasting service (sound)
BT	Broadcasting service (television)
F	Fixed service
M	Mobile, radiodetermination, amateur and related satellite services
P	**Radiowave propagation**
RA	Radio astronomy
RS	Remote sensing systems
S	Fixed-satellite service
SA	Space applications and meteorology
SF	Frequency sharing and coordination between fixed-satellite and fixed service systems
SM	Spectrum management
SNG	Satellite news gathering
TF	Time signals and frequency standards emissions
V	Vocabulary and related subjects

</div>

Note: *This ITU-R Recommendation was approved in English under the procedure detailed in Resolution ITU-R 1.*

Electronic Publication
Geneva, 2017

© ITU 2017

RECOMMENDATION ITU-R P.619-3

Propagation data required for the evaluation of interference between stations in space and those on the surface of the Earth

(Question ITU-R 208/3)

(1986-1990-1992-06/2017-12/2017)

Scope

This Recommendation provides methods for predicting signal propagation losses for interfering signals between stations in space and stations on (or near to) the surface of the Earth in the overall frequency range of 100 MHz to 100 GHz, except for a few exceptions restricted to lower frequencies which will be specified where they are described. Prediction methods for some of the loss mechanisms are reliable over narrower frequency ranges, and some of the loss mechanisms are not significant at certain frequency ranges. This Recommendation provides methods to predict the propagation losses not exceeded for 0.001%-50% of the time. Guidance is given for single entry as well as multiple entry propagation losses in analyses that determine interfering signals, where correlations of temporal variability and location variability may be influential.

Keywords

Interference, depolarization, beam spreading, scintillation, diffraction, ducting

The ITU Radiocommunication Assembly,

considering

a) that for the assessment of interference between stations based in space and those on the surface of the Earth, it is necessary to have propagation data and prediction methods that take account of atmospheric factors, and in some cases terrain, building penetration, multipath and clutter;

b) that, given the many possible applications of such evaluation, guidance is required for the selection of appropriate methods;

c) that certain analyses of potential or actual interference may need to determine the aggregate total interfering signal from numerous transmitters,

noting

a) that Recommendation ITU-R P.526 provides calculation methods for obstacle diffraction;

b) that Recommendation ITU-R P.531 provides propagation data and prediction methods for ionospheric effects on Earth-space paths;

c) that Recommendation ITU-R P.618 provides guidance on the planning of Earth-space links;

d) that Recommendation ITU-R P.676 provides methods for calculating attenuation by atmospheric gasses;

e) that Recommendation ITU-R P.834 provides information and calculation methods for the effects of tropospheric refraction;

f) that Recommendation ITU-R P.836 provides information and calculation methods for the water-vapour content of the atmosphere, including its temporal variability;

g) that Recommendation ITU-R P.2040 provides information on the interaction of radio waves with buildings,

recommends

that the guidance in Annex 1 be used for the assessment of interference between stations based in space and those on the surface of the Earth.

Annex 1

1   Introduction

This Recommendation provides guidance and calculation methods to evaluate interference between a station in space and a station on the surface of the Earth. The phrase "on the surface of the Earth" is intended to cover antennas which are within the atmosphere and not at a great height above the surface, including those installed on radio towers, buildings, land vehicles, or hand-held. This Earth-based station may be part of a satellite or terrestrial radio system. For brevity, it is sometimes referred to as the "Earth-based station".

The phrase "Earth-space" path refers to the path of radio energy between antennas in either the Earth-to-space or the space-to-Earth direction.

All propagation mechanisms are reciprocal with respect to direction unless stated otherwise.

1.1   Temporal and location variability

Many propagation losses vary in time, and with the location of Earth-based stations, particularly those located on the surface of the Earth.

Many interference analyses are "statistical" and need to consider potential temporal and spatial variabilities. If a complete cumulative distribution function of Earth-space basic transmission loss is needed, Recommendation ITU-R P.618 should be used for losses exceeded for percentages of time less than 50%. Attenuations and signal power enhancements caused by individual propagation mechanisms on an individual signal path may be treated as independent variables in many cases. Likewise, in analyses where carrier-to-(noise + interference) ratio is a figure-of-merit, interfering and desired signal power and depolarization effects may be treated as independent variables except for where the desired and interfering signal paths are physically near one another or overlapping and thus have a high degree of correlation.

For certain scenarios, there may be a degree of correlation among propagation losses on the interfering signal paths which can be accounted for by selection of the appropriate methods.

1.2   Apparent and free-space elevation angles

The elevation angle of the ray at an Earth-based station to a station in space is higher than it would be in the absence of any atmosphere, due to atmospheric refractivity. Account should be taken of this effect, particularly at low elevation angles.

The elevation angle which would exist in the absence of any atmosphere is referred as the "free-space" elevation angle, and has the symbol θ_0. The actual angle of the radio path at the Earth-based station, including the effect of atmospheric refractivity, is referred to as the "apparent" elevation angle, and has the symbol θ.

Attachment B gives methods to convert between free-space and apparent elevation angles.

1.3 Relevant propagation mechanisms

The principal basic transmission loss mechanisms on interfering signal paths occur during clear-air conditions and may include in some cases, tropospheric and ionospheric scintillation, multipath, and mechanisms associated with signal path obstructions (clutter, diffraction over terrain, and building entry loss). Section 2 describes these mechanisms and gives calculation methods. Sub-sections 2.1 to 2.8 describe the mechanisms in detail. Section 3.1 gives the expression for basic transmission loss for a single specific path. Section 3.2 gives the expression for basic transmission loss for multiple sources into a single receiver.

Some evaluations of interference may need to take precipitation effects into account. The relevant mechanisms are described in § 3. Sub-sections 2.9 and 2.10 give information and calculation methods for interference caused by rain scattering, and differential rain attenuation, respectively.

These mechanisms are considered below and are applied to determine propagation losses that are not exceeded for 50% and smaller percentages of time that are of particular interest in interference analyses.

Section 4 discusses correlation between propagation mechanisms.

2 Propagation mechanisms

The following sub-sections summarise the mechanisms which in combination determine the attenuation between the (interfering) transmitter and (interfered-with) receiver antennas, with the associated symbols to be used in equations. This overall loss is expressed as basic transmission loss, which is the loss which would occur between ideal isotropic antennas.

2.1 Free space basic transmission loss L_{bfs} (dB)

This is the basic transmission loss assuming the complete radio path is in a vacuum with no obstruction. It depends only on the path length, d (km), and frequency, f (GHz) according to

$$L_{bfs} = 92.45 + 20 \log(f \cdot d) \qquad \text{(dB)} \qquad (1)$$

Attachment A gives a method for calculating the length of an Earth-space path, and the free-space elevation angle at the Earth-based station. It is based on spherical Earth geometry, and ignores the effect of atmospheric refraction. The associated errors are not significant for calculating free-space transmission loss from the path length. L_{bfs} must always be included in the calculation of loss over an Earth-space path. It is valid for any frequency and over any Earth-space path length.

Attachment B gives methods for converting between the free-space elevation angle and the apparent elevation angle at the Earth-based station.

The method in Attachment A takes no account of any obstruction by the Earth or objects upon it such as buildings. Attachment E gives a method for testing an Earth-space path for obstructions. Diffraction loss due to obstructions is discussed in § 2.6.

2.2 Depolarization attenuation A_{xp} (dB)

Two propagation mechanisms can cause the polarization angle of a radio signal to change:

i)   Faraday rotation;

ii)   Hydrometeor scattering.

Polarization mismatch may also be attributed to antenna mismatch without rotation due to propagation effects. This is not considered in this recommendation since it involves system considerations rather than propagation.

Depolarization effects can be caused either by Faraday rotation or by precipitation scatter. Faraday rotation is only significant below 10 GHz and can be ignored for frequencies at or above 10 GHz. Depolarization loss can be significant in reducing interference. For most multiple-entry Earth-space interference situations where relative polarization orientations can be considered arbitrary, $A_{xp} = 3$ (dB) assumes that the transmitter and receiver polarization vectors are in the same plane with a uniform distribution of relative angles. In practice the polarization vectors will be arbitrarily oriented in three-dimensional space which would combine to a higher aggregated loss. $A_{xp} = 3$ (dB) is thus unlikely to over-estimate the loss.

The polarization discrimination from a space-based interference source received by an earth-based station (or vice-versa) depends on the polarization purity of the transmitted wave, as well as the cross-polarization isolation of the receiving antenna. The depolarization loss can be directly calculated in terms of parameters that describe the interfering and receiving antennas' respective polarization types and polarization purities such as axial ratio in the case of circular polarization or linear cross-polarization isolation in the case of linear polarization. In addition, the polarization sense and tilt angle of the incident wave and the receiving antenna, will act to further reduce the net depolarization loss when the actual interfering and interfered-with system parameters are taken into account.

2.2.1   Cross-polar discrimination and cross polar attenuation

Polarization mismatch can occur for several reasons, and are sometimes quantified in terms of cross-polar discrimination (XPD) which is defined as the ratio of co-polar to cross-polar signal strength, normally expressed in decibels. It is a figure-of-merit where frequency sharing is implemented by orthogonal linear polarization.

Any degradation of XPD transfers a proportion of the power to the orthogonal polarization, which can constitute a source of interference. There is a corresponding attenuation of the original signal.
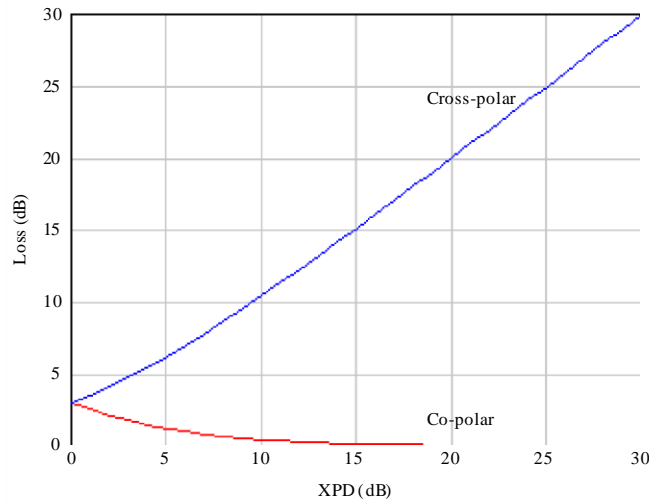
Cross- and co-polar attenuations are given by:

$$A_x = 10\log(1 + 10^{0.1R_{xpd}}) \qquad \text{(dB)} \qquad\qquad (2a)$$

$$A_c = 10\log(1 + 10^{-0.1R_{xpd}}) \qquad \text{(dB)} \qquad\qquad (2b)$$

where R_{xpd} is the XPD ratio in dB.

Figure 1 shows co-polar and cross-polar attenuation plotted against XPD.

FIGURE 1

Co- and cross-polar losses versus XPD

P.0619-01

Usually space borne RF systems employ signals with specified polarization depending on their functions. For instance tracking systems, air traffic control systems, and communication systems use vertically polarized signals to minimize interference due to reflection from ground surface.

Land surface remote sensing systems use horizontal polarization to ensure maximum coupling of the transmitted signals with ground surface. Those systems also use different polarizations to get auxiliary detail information. GNSS systems use circularly polarized signals to avoid impacts of Faraday rotation and to relax any restriction on the polarization direction of receiver antennas. Accordingly, it is important to assess values of RF signals with a specified polarization along a specified propagation path. Any reduction in those values can be considered a loss.
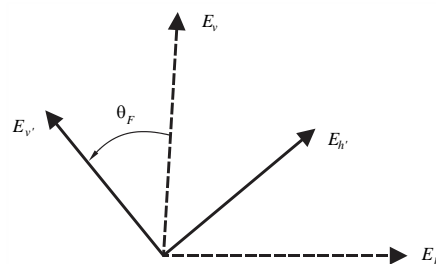
2.2.2 Faraday rotation

A linearly polarized field propagating through the ionosphere rotates from its initial direction by Faraday rotation angle θ_F. This means that the field can be split into two components:

i)   One component oriented along direction of initial polarization and having value proportional to $\cos \theta_F$;

ii)   Another component orthogonal to the initial direction and having a value proportional to $\sin \theta_F$.

Figure 2 illustrates transmitted linearly-polarized orthogonal field vectors $(\overrightarrow{E_v}, \overrightarrow{E_h})$ undergoing Faraday rotation to produce received orthogonal vectors $(\overrightarrow{E_v'}, \overrightarrow{E_h'})$.

FIGURE 2

Faraday rotation in the plane normal to the propagation direction

P.0619-02

Cross- and co-polar attenuations, A_{xF} and A_{cF} , respectively, due to Faraday rotation are given by:

$$A_{xF} = -20\log[\cos(\theta_F)] \qquad \text{(dB)} \qquad \text{(3a)}$$

$$A_{cF} = -20\log[\sin(\theta_F)] \qquad \text{(dB)} \qquad \text{(3b)}$$

where the Faraday rotation angle θ_F is given by:

$$\theta_F = 2.36 \times 10^{-14} \frac{B_{av}N_T}{f^2} \qquad \text{(rad)} \qquad \text{(4)}$$

where:

f: frequency (GHz)

N_T: total electron density (electrons m^{-2})

B_{av}: Earth's magnetic field (Tesla)

noting that $A_{xF} \to \infty$ as $\theta_F \to (2n+1)\pi/2$ for $n = 0,1,2,...$

and that $A_{cF} \to \infty$ as $\theta_F \to 2n\pi$ for $n = 0,1,2,...$.

Typical values for θ_F are given in Fig. 1 of Recommendation ITU-R P.531-13.

The matrix equation (5) can be used to recover values of transmitted linearly polarized vectors (E_v, E_h) from the corresponding received values (E_v', E_h') after undergoing Faraday rotation.

$$\begin{bmatrix} E_v \\ E_h \end{bmatrix} = \begin{bmatrix} \cos\theta_F & \sin\theta_F \\ -\sin\theta_F & \cos\theta_F \end{bmatrix} \begin{bmatrix} E_v' \\ E_h' \end{bmatrix} \qquad \text{(5)}$$

2.2.3 Hydrometeor depolarization

Hydrometeor depolarization is another way of changing the polarization of RF signals, and hence leading to depolarization loss. Hydrometeor depolarization is usually described by the cross polarization discrimination ratio XPD which is the ratio of the power with the expected polarization to the power with the orthogonal polarization in dB units as reported in Recommendation ITU-R P.310.

The polarization discrimination ratio is used as a measure of the degree of interference between orthogonally-polarized channels and it reaches ∞ dB when the power with orthogonal polarization reaches zero. On the other hand, XPD values reach $-\infty$ dB when power with expected polarization has null values.

By considering the expected polarization direction q as the direction of like polarization, the propagation loss factor A_{xq} due to hydrometeor depolarization can be written as:

$$A_{xq} = -20 \log \left\{ \cos \left(\tan^{-1} \left\{ 10^{\frac{-XPD_q}{20}} \right\} \right) \right\}, \qquad q = v, h, c \qquad \text{(6)}$$

In the above, v , h , and c stand for vertical polarization, horizontal polarization, and circular polarization respectively. Based on equation (6), when the polarization of propagating signal align along expected polarization direction, $XPD_q \to \infty$, and $A_{xq} \to 0$. On the other hand, when polarization of propagating signal is orthogonal to direction of expected polarization, $XPD_q \to -\infty$, and $A_{xq} \to \infty$.

XPD_q in equation (6) can be obtained from § 4.1 of Recommendation ITU-R P.618-12 by setting the proper value of the polarization angle τ in equation (70) of Recommendation ITU-R P.618-12. For instance, in case of vertical polarization, to $\tau = \pi/2$ and in case of horizontal polarization $\tau = 0$. The current ITU-R Depolarization Prediction Procedure in Recommendation ITU-R P.618 does include a term which accounts for additional XPD due to ice particle depolarization. The ITU procedure determines the XPD due to rain from the copular attenuation (either measured or calculated

from the ITU-R Rain Attenuation Prediction Procedure in Recommendation ITU-R P.618). Then an additional *XPD* degradation due to ice particles in the path is determined by an empirical estimate based on the statistics of ice depolarization as related to coincident rain depolarization.

2.3 Attenuation due to atmospheric gasses A_g (dB)

The attenuation due to absorption by atmospheric gasses, A_g (dB), is a complicated function of frequency, according to the varying attenuation rates of oxygen and water vapour with frequency as described in Recommendation ITU-R P.676.

The attenuation increases as path elevation angle decreases, due to the longer path in the atmosphere, and decreases with the altitude of the Earth-based station, due to the shorter path in the atmosphere and its lower density.

At many frequencies water-vapour is the dominant cause of attenuation. At such frequencies, in addition to the foregoing geometrical factors, there is both spatial and temporal variability of the attenuation due to water-vapour density, which varies with location and weather.

Recommendation ITU-R P.836 provides digital global maps of surface water-vapour density exceeded for a range of percentage times of an average year or of a month at a given location.

Recommendation ITU-R P.453 gives expressions relating water-vapour density and relative humidity. The highest possible water-vapour density at any time and location is limited to the value corresponding to 100% relative humidity. Some of the higher values of water-vapour density in the Recommendation ITU-R P.836 data maps are only possible at temperatures well above local annual mean values.

Attachment C gives a method for calculating the attenuation due to atmospheric gasses. The calculation takes the altitude of the Earth-based station into account, and is extended for ray elevation angles down to −2 degrees. Although negative apparent ray elevation angles would not normally be considered for a wanted Earth-space link, such a path might be significant when evaluating interference.
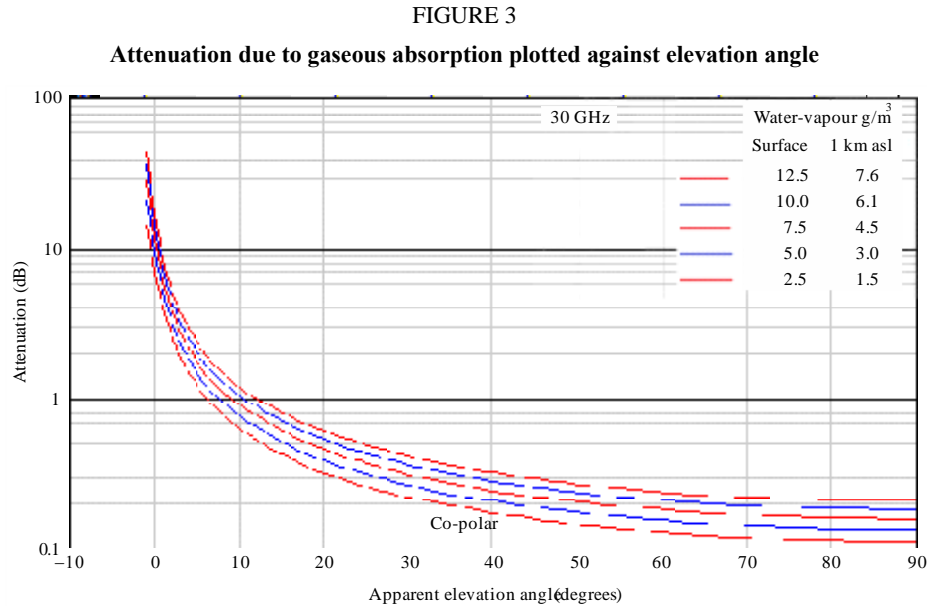
Attachment A gives a method for calculating the free-space elevation angle.

Attachment B gives a method for calculating the apparent elevation angle given the free-space elevation angle.

The method in Attachment C is valid over the frequency range 1 GHz to 1 000 GHz. Gaseous attenuation can be ignored below 1 GHz. For large values of elevation angle, in some situations, it might be valid to ignore gaseous attenuation at somewhat higher frequencies.

Figure 3 gives examples of results from the method in Attachment C for an Earth-based station at a ground and station altitude of 1 km above sea level. Total gaseous attenuation in dB is plotted against apparent elevation angle for a frequency of 30 GHz, for five values of sea-level water-vapour density, 7.5 g/m^3 being the reference global mean. The corresponding surface water-vapour densities at the ground level of 1 km above sea level ρ for this calculation are obtained by the scaling according to $\rho = \rho_0 exp\left(\frac{-h}{2}\right)$ g/m^3 where ρ_0 g/m^3 is the sea-level surface density. The Figure illustrates this effect of altitude on water-vapour density by listing their values at both sea level and 1 km above sea level.

Figure 3 demonstrates the rapid rise of gaseous attenuation as the elevation angle decreases towards zero. The attenuation on Earth-space paths is sometimes assumed to be negligible below about 10 GHz. This may not be true for paths with low elevation angles. For elevation angles below about 10 degrees it is recommended that the calculation is performed for any frequency above 1 GHz.

FIGURE 3

Attenuation due to gaseous absorption plotted against elevation angle

P.0619-03

2.4 Loss due to beam spreading A_{bs} (dB)

Refractive effects in the atmosphere result in the apparent elevation angle at an Earth-based station being higher than the elevation angle of the straight line to the space station, especially at low elevation angles. The effect is small above about 5 degrees, but can be significant for lower elevation angles. Attachment B gives methods for converting between these two elevation angles.

Sub-section 2.4.1 described atmospheric effects which cause ray bending.

Sub-section 2.4.2 gives a method for calculation the attenuation or enhancement due to de-focussing or focusing caused by atmospheric refractivity.

2.4.1 Ray bending

The following sub-sections, 2.4.1.1 and 2.4.1.2, describe the two mechanisms causing atmospheric refraction, tropospheric and ionospheric.

2.4.1.1 Tropospheric refraction

The frequency independent variations are stemming from variations of the pressure, P, water vapour pressure e, and temperature T, and it is given by:

$$n = 1 + 10^{-6} \times N = 1 + 10^{-6} \times \left[\frac{77.6}{T} \left(p + e + 4810 \frac{e}{T} \right) \right] \tag{7}$$

In the above N is the refractivity, P and e are in hPa units, and T is in Kelvin. In addition, equation (7) can be applied at frequencies up to 100 GHz.

The frequency dependence variations are attributed to the absorption spectral lines of atmospheric gasses, especially oxygen and water vapour. Contributions of those spectral lines to the atmospheric refractive index can be obtained from Recommendation ITU-R P.676-11 and they can be ignored at frequencies below 10 GHz.

For ease of geometrical analysis, the tropospheric refracted rays can be represented as straight lines then compensation is done by assuming an imaginary earth radius, otherwise referred to as effective earth radius, R_e. The ratio between the effective R_e and true earth radius a is referred to as the effective earth radius factor (k-factor) and is given by:

$$k = \frac{R_e}{a} = 1 + a\frac{dn}{dh} = \frac{1}{1 + \frac{dN/dh}{157}} \tag{8}$$

with $\frac{dn}{dh}$ is the refractive index gradient with atmospheric height h.

Depending on k-factor value, the tropospheric refraction can be characterized as normal refraction, sub-refraction, super-refraction and ducting as shown in Fig. 4 and explained below.

FIGURE 4

Tropospheric refraction
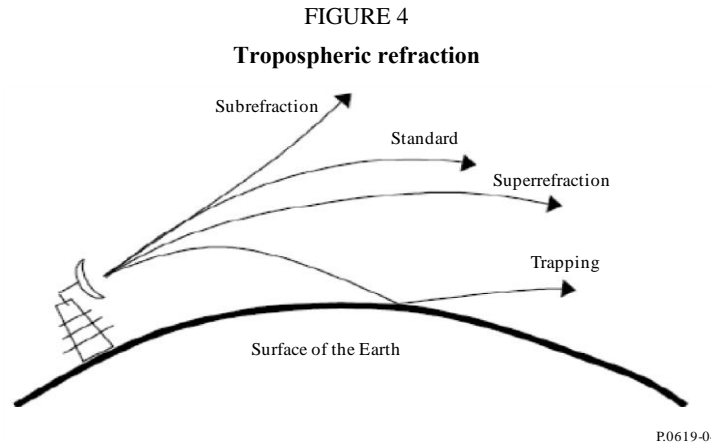
When:

$$k = \frac{4}{3} \tag{9a}$$

Normal refraction occurs, and RF rays travel on a straight line path along the earth's surface and go out to space unobstructed.

If:

$$\frac{4}{3} > k > 0 \tag{9b}$$

sub-refraction occurs, meaning that radio waves propagate away from the earth's surface.

When:

$$\infty > k > \frac{4}{3} \tag{9c}$$

super-refraction occurs and RF rays propagate towards the earth's surface thus extending the radio horizon.

Finally, if:

$$-\infty < k < 0 \tag{9d}$$

ducting occurs and the RF rays bend downwards with a curvature greater than that of the earth. This is also called trapping.

2.4.1.2   Ionospheric refraction

Figure 5 provides examples of ray signals transmitted at different frequencies by a transmitter located on the ground surface. Rays propagating at vertical incidence into the ionosphere with frequencies above the maximum critical frequency $(foF2)$ of the F2 ionospheric layer, pass through the ionosphere. If the propagation direction of those rays deviates away from the vertical incidence direction, the rays undergo refraction before passing through the ionosphere as shown by ray 4 and ray 5 in Fig. 5. Some of those rays may be refracted enough to be reflected back to the ground as shown by ray 6 in Fig. 5.

Rays propagated obliquely into the ionosphere at frequencies below $foF2$ are refracted and can be reflected back to the ground after a skip distance depending on both the (oblique) initial elevation angle of the rays, and the frequency as illustrated by ray 2 and ray 3 in Fig. 5. Moreover, rays propagating with frequencies below the plasma frequency at the bottom of the lower ionospheric layer, the E layer, are reflected back to the ground at the bottom of the E layer as shown by ray 1 in Fig. 5.
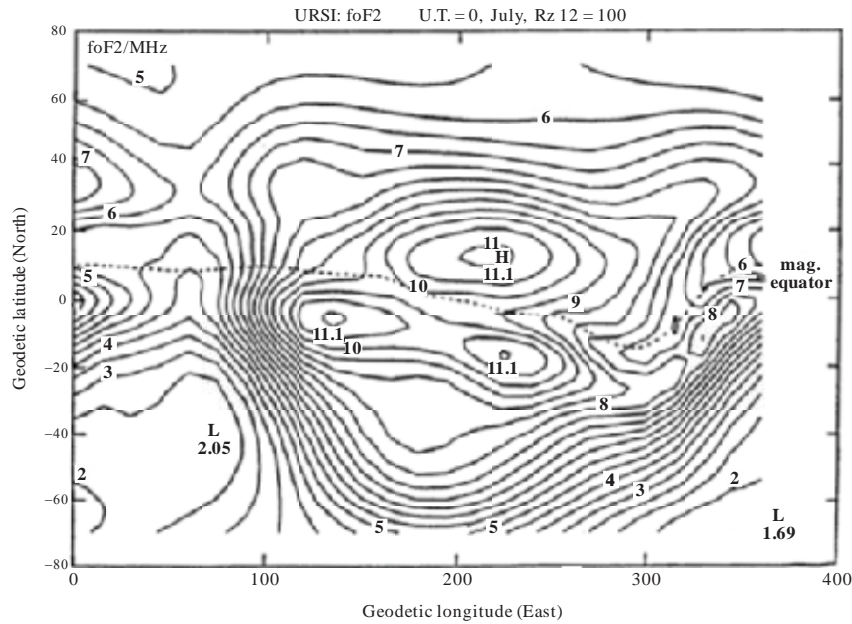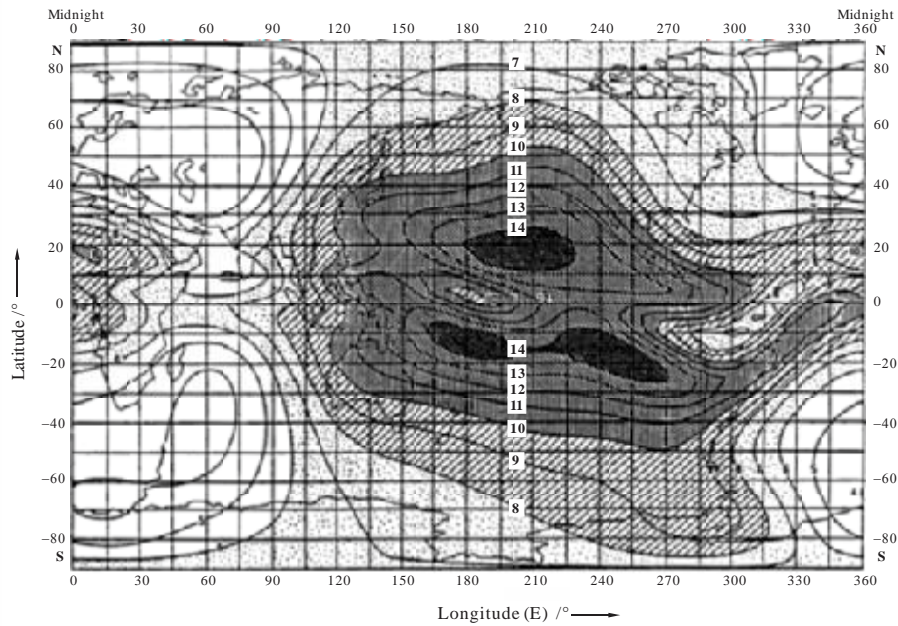
FIGURE 5

Ionospheric refraction
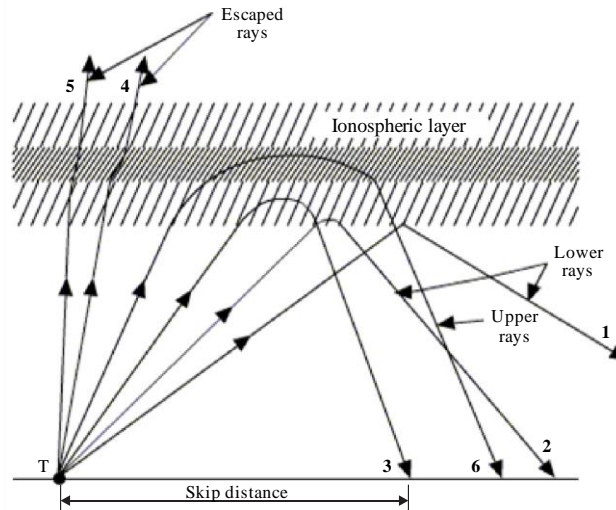
P.0619-05

Figure 6 shows an example of the global distribution for $foF2$ for a time corresponding to 0 UT, for the month of July, for sunspot number 100.

FIGURE 6

Ionospheric refraction

2.4.2 **Beam-spreading loss for propagation through the atmosphere**

Beam spreading loss, A_{bs}, is a non-ohmic loss due to spreading of the antenna beam in the vertical elevation plane due to the variation of the radio refractive index vs. height. This effect is insignificant for elevation angles above 5 degrees.

The signal loss due to beam spreading for a wave propagating through the total atmosphere in the Earth-space and space-Earth directions is:

$$A_{bs} = \pm 10\log(B) \qquad \text{(dB)} \qquad (10)$$

where:

$$B = 1 - \frac{0.5411 + 0.07446\theta_o + h(0.06272 + 0.0276\theta_o) + h^2 0.008288}{\left[1.728 + 0.5411\theta_o + 0.03723\theta_o{}^2 + h(0.1815 + 0.06272\theta_o + 0.0138\theta_o{}^2) + h^2(0.01727 + 0.008288\theta_o)\right]^2} \qquad (10a)$$

where:

θ_0: elevation angle of the line connecting the transmitting and receiving points (degrees) ($\theta_0 < 10°$)

h: altitude of the lower point above sea level (km) ($h \leq 5$ km).

Figure 7 shows the beam spreading loss vs. the free-space elevation angle for altitudes of the lower point above sea level of 0, 0.5, 1, 2, 3 and 5 km. The magnitude of the beam-spreading loss is independent of frequency over the range of 1–100 GHz.

FIGURE 7

Beam spreading loss in both the Earth-to-space and space-to-Earth directions

P.0619-07
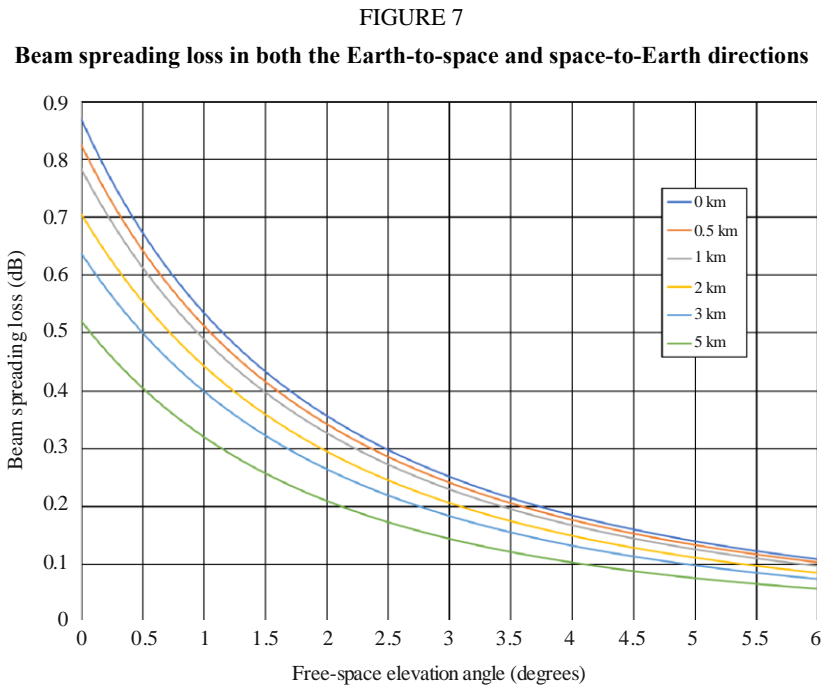
2.5 Scintillation

Two different mechanisms on Earth-space paths result in signal-level fluctuations which change rapidly in time and over short distances. The two mechanisms are effectively over mutually exclusive frequency ranges, as outlined in the following sub-sections, and thus normally only one needs to be considered for a particular case. Scintillation is formulated here as an attenuation. Each individually must be treated as variable in time, with zero at the median of each distribution. Thus scintillation attenuation (dB) varies between positive and negative values. When many unwanted signals are aggregated at a victim receiver, scintillations will effectively cancel and the mechanism can be ignored.

2.5.1 Ionospheric scintillation A_{si} (dB)

Recommendation ITU-R P.531 contains propagation data and calculation methods for predicting the effect of ionospheric scintillation. The effect on signal level decreases with frequency. It is rarely significant above 10 GHz and can be ignored above this frequency.

2.5.2 Tropospheric scintillation A_{st} (dB)

This section gives a method for calculating the effect of tropospheric scintillation.

Variations in refractive index caused by atmospheric turbulence can cause spatial and temporal fades and enhancements in signal strength. The physical process consists of alternating focussing and

defocusing of a radio wave. The strength of these scintillations correlates well with the wet term of the atmospheric refractive index, which is related to water-vapour density.

The general strength of tropospheric scintillation thus varies on spatial and temporal scales typical of water-vapour density, typically at least tens of kilometres and hours. The actual scintillations occur at much smaller scales, typically less than a wavelength and in seconds.
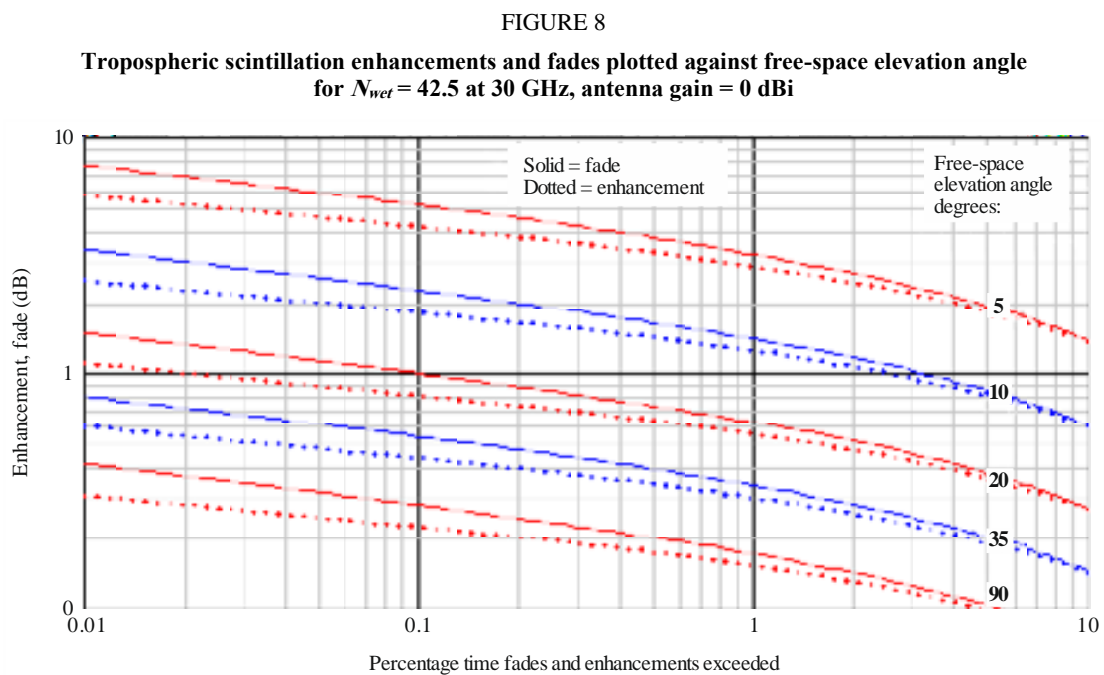
The statistical distribution of signal strength variability, when expressed in dB is not symmetrical, with the fade exceeded for a given percentage time greater than the enhancement exceeded for the same percentage time. This asymmetry in the signal-strength variability is greatest in the tails of the distribution.

Since the mechanism consists only of focussing and defocusing, not the absorption of energy, the net effect of tropospheric scintillation, when averaged over space and/or time, tends to zero. It is thus significant when considering single-entry interference and in the case of short-term effects, but tends to cancel in the multiple-entry, long-term interference case when the aggregated signals each have similar average strength.

The spatial averaging of scintillation also tends to reduce its significance when the diameter of an antenna's effective aperture is comparable or larger than the spatial correlation distance. Attachment D gives a calculation method to predict the strength and temporal distribution for both enhancements and fades. The enhancement exceeded for percentage time p is expressed as $E_{st}(p)$ (dB). $E_{st}(p)$ is negative for $p > 50$, representing a fade. The underlying method is the same as given in § 2.4.1 of Annex 1 to Recommendation ITU-R P.618 for an Earth-space link, but has been extended to cover both enhancements and fades.

The tropospheric scintillation effect can be considered negligible below 4 GHz. This model is based on measurements up to 20 GHz. Considering the underlying physics, this model is thought to be reliable up to about 100 GHz. The model is accurate for angles from 4 to 90 degrees.

Figure 8 gives examples calculated by the method in Attachment D.

FIGURE 8

Tropospheric scintillation enhancements and fades plotted against free-space elevation angle for N_{wet} = 42.5 at 30 GHz, antenna gain = 0 dBi

P.0619-08

2.6   Diffraction/ducting loss due to terrain and/or specific obstruction L_{dtb} (dB)

The following method calculates diffraction loss due to terrain or obstruction at the Earth-based station by a specific building or other surface object, taking ray-bending into account. Since diffraction loss varies with the atmospheric refractivity gradient, L_{dtb} has temporal variability. The method constructs a ray-traced path through the atmosphere to take account of typical refractivity conditions. Since distances between the Earth-based station and obstacles such as buildings are likely to be short relative to the path through the atmosphere, variations in refractivity gradient will have little effect. Diffraction losses due to terrain obstruction are more likely to be influenced by atmospheric conditions. The method includes a reduction to diffraction loss to account for ducting. Ducting exists only in the lowest layers of the atmosphere. For a low-angle Earth-space path, any duct can form only a very small fraction of the total path length. Thus ducting enhancements on a low-angle Earth-space path which is not obstructed by terrain will be negligible. Also, ducting enhancements do not occur when obstructed by clutter (e.g. buildings in an urban environment).

The calculation is valid for frequencies up to 100 GHz. L_{dtb} should be set to zero if the Earth-based station has no terrain or other obstruction, either because the environment is uncluttered or the path elevation is high enough to avoid obstruction.

Earth-space paths may be obstructed by terrain or buildings for low apparent elevation angles. Recommendation ITU-R P.834 provides a method for predicting the visibility of a space station taking atmospheric refraction into account for a smooth uncluttered spherical Earth. If it is wished to take actual terrain and possibly other obstacles into account, such as for Monte-Carlo simulation, the ray-tracing method given in Attachment E gives a profile of the ray height relative to sea level, independent of frequency up to 100 GHz.

Diffraction loss starts to be significant when an obstacle enters the first Fresnel zone of a radio ray. Diffraction models are given in Recommendation ITU-R P.526 suitable for a variety of situations. Many of these models are based on a dimensionless parameter, ν, to represent the obstruction geometry. The radius of the first Fresnel zone at the obstruction, R_1, is also significant, since for a single dominant obstruction, having 0.6 of this radius unobstructed around the ray is a widely-used criterion for negligible diffraction loss.

The expressions for ν and R_1 are simplified when the distance to one terminal is much less than to the other, which will be true for a ground-based obstruction on an Earth-space path. Under these conditions the two parameters are well approximated, in self-consistent units, by:

$$v \approx h\sqrt{\frac{2}{\lambda d}} \qquad\qquad (11a)$$

$$R_1 \approx \sqrt{\lambda d} \qquad\qquad (11b)$$

where h is the obstruction height relative to the ray, λ is the wavelength, and d is the distance from the Earth-based station to the obstruction, or in practical units by:

$$v \approx 0.08168h\sqrt{\frac{f}{d}} \qquad\qquad (12a)$$

$$R_1 \approx 17.314\sqrt{\frac{d}{f}} \qquad (m) \qquad\qquad (12b)$$

where obstruction height h is in metres, frequency f is in GHz, and distance d is in km.

Figure 9 shows examples of the geometry associated with R_1 and h at the Earth end of an Earth-space path. The curved red line traces a ray launched from 50 metres above sea level at an elevation angle of minus 0.1 degrees plotted with its height relative to sea level. Sea level is plotted as though flat, and the curve of the red trace takes both Earth curvature and atmospheric refraction into account.

At 24 km from the Earth-based station a hypothetical obstacle is plotted in brown with its top at 100 metres above sea level. The ray height at this point is 39.7 metres, and thus the obstacle height, h, is 60.3 metres. The corresponding diffraction parameter ν is about 4.9.

At 30 km from the Earth-based station the first Fresnel radius F_1 at 30 GHz is about 17 metres, plotted in blue both above and below the ray. For negligible diffraction loss, 0.6 of the radius should be unobstructed in a circle around the ray.

Comparing the obstacle height h in this example with F_1, and noting that F_1 would be slightly smaller at 24 km, makes it clear that the ray would be heavily obstructed in this example.

FIGURE 9

Geometry of diffraction parameters in relation to Earth-space ray
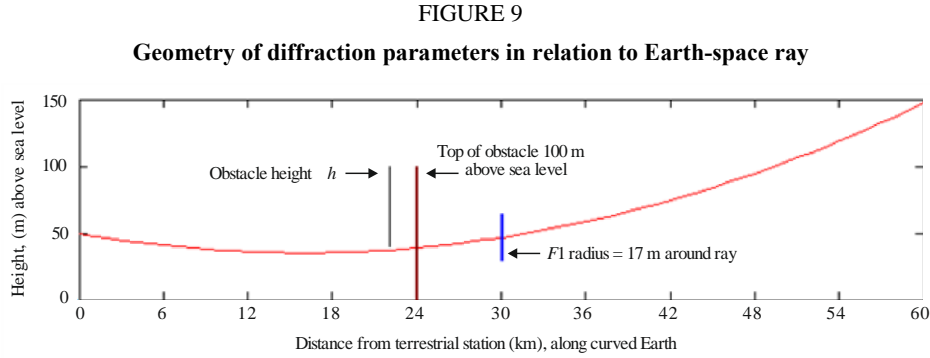
P.0619-09

For terrain obstruction, where the obstacle width can be assumed to be wide in the horizontal sense compared with the Fresnel zone, the formulation for knife-edge diffraction in Recommendation ITU-R P.526 is an appropriate model for diffraction loss.

The geometry of obstruction by a building can be more complicated. For an isolated structure a lower-loss path may exist to the left or right rather than over the obstruction. If this is possible, the finite-width model in Recommendation ITU-R P.526 is recommended. It is formulated in a variety of forms, including one intended for an unwanted path.

The knife-edge and finite-width diffraction models scale accurately with frequency, and are applicable up to 100 GHz. In the upper part of this frequency range the wavelength is only a few millimetres. As a result, the transition between unobstructed propagation and large diffraction losses become so small that accuracy of the result depends mainly on the quality of topographic data.

In cases where L_{dtb} is calculated for terrain obstruction, the value not exceeded for $p\%$ time taking atmospheric ducting at low angles into account is calculated as given by:

$$L_{dtb}(p) = \begin{cases} \max[L_d + A(p) + A_{ds}, 0] & p < \beta \\ L_{dtb} & \text{otherwise} \end{cases} \quad \text{(dB)} \quad (13)$$

where:

$$A(p) = \begin{cases} (1.2 + 3.7 \times 10^{-3}d)\log\left(\frac{p}{\beta}\right) + 12\left[\left(\frac{p}{\beta}\right)^{\Gamma} - 1\right] & p < \beta \\ 0 & \text{otherwise} \end{cases} \quad \text{(dB)} \quad (13a)$$

$$\Gamma = \frac{1.076}{[2.0058 - log(\beta)]^{1.012}} \exp\{-[9.51 - 4.8\log\beta + 0.198(\log\beta)^2]\} \quad (13b)$$

$$\beta = \begin{cases} \left(10^{-0.015|\varphi|} + 1.67\right) & \text{for } |\varphi| \leq 70 \\ 4.17 & \text{otherwise} \end{cases} \quad (\%) \quad (13c)$$

$$A_{ds} = \begin{cases} 20\log[1 + 0.361\theta''(f \cdot d_{hoz})^2] + 0.264\theta''f^{1/3} & \theta'' > 0 \\ 0 & \text{otherwise} \end{cases} \quad \text{(dB)} \quad (13d)$$

$$\theta'' = \theta_{hoz} - 0.1 d_{hoz} \qquad \text{(mrad)} \qquad (13e)$$

L_d: diffraction loss due to a local obstruction calculated using Recommendation ITU-R P.526, for a single knife-edge obstacle $J(v)$ or for a finite-width screen $J_{min}(v)$

φ: latitude (degrees)

f: frequency (GHz)

θ_{hoz}:   elevation angle of the Earth-based station's horizon above horizontal (mrad)

d_{hoz}:   the horizon distance of the Earth-based station (km)

and noting that $A(p)$ is negative when $p < \beta$.

2.7   Clutter loss L_c (dB)

The overall Earth-space basic transmission loss for an Earth-based station below roof-top level in an urban environment will in general be modified by the station's surroundings. The loss may be increased by diffraction due to obstructions, or reduced by the existence of reflection paths. The dominant source of obstruction and reflecting surfaces consists of buildings, but other types of artificial structure may be involved. Vegetation can also cause additional loss, although the variable nature of vegetation means that it is not normally considered a reliable basis for predicting loss on an interference path.

In the case of a specific Earth-based station where data exists on its surrounding, it is more appropriate to calculate diffraction loss L_{dtb} for either terrain or urban obstructions, as described in § 2.6 above. If a reflection path also exists, this can be taken into account using information contained in Recommendation ITU-R P.2040.

In the case of the area deployment of many Earth-based stations, either real or representative, it is not normally practicable to perform detailed calculations for each. The actual clutter loss for Earth-based stations within urban clutter varies greatly between individual locations, as well as with the direction of the Earth-space path. For this reason, it may be more appropriate to use a statistical approach where representative models (e.g. using a combination of clutter heights and distances) are used according to the physical environment being modelled. A statistical approach is typically used in a Monte-Carlo simulation. Recommendation ITU-R P.2108-0 gives a suitable clutter-loss model for this purpose.

2.8   Building entry/exit loss L_{be} (dB)

For an indoor Earth-based station, account must be taken of the additional loss between the station and the adjacent outdoor path. As for L_c , L_{be} varies greatly with the location and construction details of buildings, and a statistical evaluation is required. Recommendation ITU-R P.2109-0 gives a suitable building entry/exit-loss model for this purpose.

2.9   Precipitation-scatter transmission loss L_{tps} (dB)

Scattering by rain or other hydrometeors can produce coupling between a transmitter and a receiver which would not exist under clear-air conditions. The associated loss over such a path must be evaluated as transmission loss, since the antenna radiation pattern at both stations form an essential part of the calculation.

Interference can be caused when energy from one system is redirected or scattered by precipitation and enters the antenna beam of another system. This situation is of potential significance primarily at frequencies above 5 GHz and when the main beams of the two systems forming a common volume intersecting within that portion of the atmosphere in which hydrometeors can exist. Under these conditions, a common illuminated volume exists in which hydrometeors are present for appreciable

periods and enhanced levels of unwanted signals may result. While such interference can be significant, it is transient, and it is usually not severe enough to be system-limiting and, by a judicious selection of path geometries to prevent the likelihood of common volumes occurring, can usually be avoided altogether.

A method for calculating precipitation scatter between stations on the surface of the Earth at frequencies above about 0.1 GHz is given in Recommendation ITU-R P.452. The method can be used for a common volume formed by the beams of an antenna on the ground and an antenna in space.

Precipitation scatter is most likely to be a significant interference mechanism between two Earth-space links, both in satellite services. It is less probable when the Earth-based terminal is part of a terrestrial radio system. Since the precipitation-scatter method in Recommendation ITU-R P.452 is numerically intensive, Attachment F describes a relatively simple test which can identify cases where no risk of significant precipitation-scatter interference exists before taking the mechanism into account.

2.10 Differential rain attenuation

Attenuation due to precipitation, which includes rain, wet snow and clouds, is usually the most significant degradation mechanism for a wanted Earth-space path at frequencies above about 5 GHz. Depending on the interference analysis method, it may be useful to know the correlation between precipitation fading on both wanted and unwanted paths.

Recommendation ITU-R P.1815 gives a method for predicting the joint statistics of rain fading for the paths between two Earth-based stations each to the same space station. It gives the probability that the attenuations on the two paths exceed individual specific thresholds, given that it is raining at both sites. The calculation is based on the Earth-space rain fade model in Recommendation ITU-R P.618, which is valid up to 55 GHz.

The correlation of rain rate between two sites falls to low values over distances typical of rain cells. Intense rain often falls in cells having horizontal extents of a few kilometres, although intense frontal rain can exist over longer distances aligned with the front.

3 Evaluation of interference

The following sub-section give analysis method to be used to evaluate unwanted signal levels according to the type of interference scenario.

3.1 Basic transmission loss for single-entry interference

The clear-air basic transmission loss not exceeded for p% time for a single unwanted transmitter and victim receiver over an Earth-space path is composed of losses described in §§ 2.1 to 2.6 as follows:

$$L_b = L_{bfs} + A_{xp} + A_g(p_1) + A_{bs} + A_s(p_2) + L_{dtb}(p_1) \qquad \text{(dB)} \qquad (14)$$

where:

L_{bfs} : free space basic transmission loss

A_{xp} : attenuation due to depolarization

$A_g(p_1)$: attenuation due to atmospheric gasses not exceeded for p_1% of the time

A_{bs} : attenuation due to beam-spreading

$A_s(p_2)$: attenuation due to either ionospheric or troposcatter scintillation not exceeded for p_2% of the time, according to whether the frequency is less than or greater than 10 GHz

$L_{dtb}(p_1)$:   ducting-enhanced diffraction loss not exceeded for p_1% of the time.

and all of the above terms of equation (14) are losses (dB), noting that A_s has a zero median and can take positive or negative values.

The two clutter-related losses L_c and L_{be} are omitted from equation (14) because they are statistical results and not appropriate to a single interference path. Any losses increased by obstruction or decreased by reflection should be calculated specifically using the methods described in § 2.6. In practice it is expected that single-entry interference evaluation would involve only Earth and space stations in the satellite service. In most of such cases the Earth-based station would not be influenced by diffraction or reflection.

The use of separate symbols for percentage times p_1 and p_2 in equation (14) recognises that depending on the overall analysis method, these percentage times may have different values, as discussed in § 3.

For the special case, where p = 20-50%, the impact of scintillation on clear-air basic transmission loss is negligible. This special case is that corresponding to that what is typically treated as the long-term single-entry interference path. This case based is on ITU-R studies which have shown that for the p = 20 to 50% of the time, in the calculation of the clear-air basic transmission loss not exceeded for p% of the time, that:

$$A_g(p_1) + A_s(p_2) \approx A_g(p) \text{ for } 0.001 \leq p_1 \leq 99.999\%, 0.001 \leq p_2 \leq 99.999\% \text{ and } p = 20\text{-}50\%$$

The studies demonstrated that for elevation angles of 1° to 5°, for frequencies 24-71 GHz, over a range of varied climates, the loss of accuracy in this simplified method for the long-term case was insignificant.

3.2   Clear-air basic transmission loss for multiple-entry interference

The clear-air basic transmission loss not exceeded for p% of the time for each unwanted transmitter in a multiple-entry Earth-space interference calculation is composed of losses described in §§ 2.1 to 2.6 and §§ 2.7 and 2.8 as follows:

$$L_b = L_{bfs} + A_{xp} + A_g(p) + A_{bs} + L_c(p_{Lc}) + L_{be}(p_{Lbe}) + L_{dtb}(p) \qquad \text{(dB)} \qquad (15)$$

where:

L_{bfs}:   free space basic transmission loss

A_{xp}:   attenuation due to polarization mismatch

A_{bs}:   attenuation due to beam-spreading

$L_c(p_{Lc})$:   clutter loss not exceeded for p_{Lc} percent

$L_{be}(p_{Lbe})$:   building entry loss not exceeded for p_{Lbe} percent indoor stations, = 0 dB for an outdoors Earth-based station

$L_{dtb}(p)$:   ducting-enhanced diffraction loss not exceeded for p_3% of the time.

In this situation temporal variability is taken into account only for loss due to atmospheric gasses.

Clutter losses L_c, as specified in Recommendation ITU-R P.2108-0, and if needed building entry/exit losses L_{be} as specified in Recommendation ITU-R P.2109-0, are expressed as losses not exceeded for given percentages of locations. In multiple-entry simulations, new uniformly-distributed random values of percentage locations should be used for each loss extracted from the clutter and building entry loss (BEL) models.

The aggregated power received by the victim receiver should be calculated by the summation of power in linear units (that is, not in dB) for each path. This will approximate well to the median of the spatial distribution produced by the phasor addition of the multiple signals.

4 Correlation between propagation losses

The following general observations can be made concerning correlation between propagation mechanisms on an Earth-space path.

Losses associated with ground clutter, both its spatial and temporal variation, are largely independent of mechanisms arising in the atmosphere or over the full length of the path, except that apparent ray elevation angle depends on the vertical refractivity gradient, which can affect terrain or other obstruction loss for a low-elevation angle path.

Free-space loss, gaseous attenuation, and tropospheric scintillation intensity, all increase with decreasing path elevation angle.

The degree to which water-vapour density affects gaseous attenuation depends in a complicated manner on frequency, and is negligible in the vicinity ±10% of the 60 GHz oxygen absorption band. At other frequencies above about 5 GHz, and for a single Earth-space path for which tropospheric scintillation is significant, there will be a tendency for an increase in scintillation enhancements with water-vapour density to be counteracted by an increase in gaseous attenuation, but the relative amplitude of these two effects vary with frequency.

Gaseous attenuation and the intensity of tropospheric scintillation show partial positive correlation. Gaseous attenuation increases with water-vapour density in the atmosphere, ρ (g/m^3). Tropospheric scintillation is mainly due to atmospheric turbulence at the height of cloud formation, and the scintillation intensity correlates with the wet term of the radio refractivity N_{wet}, which increases with water-vapour density, although with a different dependency on temperature.

Attachment C describes the calculation of slant-path gaseous attenuation with surface water-vapour density ρ_o (g/m^3) as an input.

Tropospheric scintillation intensity depends on N_{wet} as given by equation (63) of Attachment D. Section 1 of Recommendation ITU-R P.453-11 gives N_{wet} as a function of water-vapour partial pressure e (hPa). Section 1.2 of Recommendation ITU-R P.835-5 gives the relationship between ρ_o and e.

A detailed analysis of the interaction between gaseous attenuation and tropospheric scintillation would require a technique such as simulation, taking weather data into account. For clear-air single-entry interference evaluation using equation (14), a good approximation to the temporal variability is obtained by setting $p_1 = p$, and setting $p_2 = 50$ which has the effect of setting $A_s = 0$ (dB). This approximation is based on the variability of scintillation loss having a zero median.

Tropospheric scintillation variability occurs over time scales of seconds, compared to the hours or greater over which gaseous attenuation varies. If this fast variation is significant to the interfered-with receiver, p_2 should be set to the required percentage of short-term time ($\leq$1%) during which $A_s p_2$ is not exceeded.

5 Multiple-entry interference analysis methods

There are two types of approaches that could be followed in treating multiple entry interference:

– Experimental approaches, or

– Theoretical approaches.

Experimental approaches are based on measured data which could be difficult or even impossible to acquire in case of deployed space station. Accordingly, theoretical approaches for treating propagation mechanisms unique to multiple entry interference are considered in this Recommendation.

There are two types of approaches for treating propagation mechanisms unique to multiple entry interference:

– Monte-Carlo simulation;

– Analytical techniques.

In both types of techniques the multiple entry interference power I_A is treated as the sum of interference powers $I_i's$ stemming from the different interferers:

$$I_A = \sum_i I_i \tag{16}$$

where summation is performed over all interferers visible to the victim receiver. The determination of the summation area depends on the coexistence scenario and is outside the scope of this Recommendation. The interference power I_i stemming from each interferer can be written as:

$$I_i = X_i \, g(d_i) \tag{17}$$

X_i is a random positive variable that can be modelled as the multiplication of deterministic quantities and various random variables reflecting several parameters including the transmit power, antenna gain, channel attenuation including all factors reported in equation (14) in linear values with adding attenuation due to precipitation if it exists. Some of those random variables could be correlated. The function $g(d_i)$ represents the distance dependent propagation loss which depends on the distribution of the individual emitters/victim receivers.

5.1 Monte Carlo simulation

Monte-Carlo simulation technique is based on calculating equation (17) for each interferer/victim numerically and summing the resultants to get the multiple entry interference power as reported in equation (16). In order to obtain the multiple entry interference power, it is necessary to characterize the propagation loss from each interferer to the victim receiver. Such a propagation loss depends on deployment conditions, terrain and on atmospheric conditions.

Equation (16), although simple, is could be difficult to apply for calculating multiple entry interference power, since the number of interferers could be very large, interferer radiated powers toward the victim receiver could in some cases be unknown, and the propagation losses in equation (17) depend on the deployment conditions, intervening terrain and the atmospheric conditions.

5.2 Analytical techniques

A statistical analytical technique can be used as an approximation to a Monte Carlo technique, e.g. the cumulant-based analytical technique. The cumulant-based analytical technique provides closed-form equations for mean and variance of the interfering power stemming from a finite distribution of emitters/receivers provided that the distribution of the emitters/receivers is known. It should be noted that distribution of emitters/receivers depends on the specific deployment scenarios of the interference/victim sources, which should be taken into account, but are not always easy to characterize.

Attachment A
to Annex 1

Geometry of straight-line Earth-space path

The following step-by-step method calculates the distance, elevation angle and azimuthal bearing of a space station as viewed from an Earth-based station. It is based on spherical Earth geometry, and ignores the effect of atmospheric refraction. The associated errors are not significant for calculating free-space transmission loss from the path length.

For other purposes the difference between free-space and apparent elevation angles may be significant. Attachment B gives methods for converting between these two angles.

The inputs to the calculation are:

H_s: Altitude of space station, (km) above sea level

H_t: Altitude of Earth-based station, (km) above sea level

φ_s: Latitude of sub-satellite point (zero for geostationary satellite)

φ_t: Latitude of Earth-based station

δ: Difference in longitude between the sub-satellite point and the Earth-based station, limited to less than half a circle, positive when the space station is to the east of the Earth-based station.

Step 1: Calculate the distances of the space station and the Earth-based station from the centre of the Earth, respectively:

$$R_s = R_e + H_s \qquad \text{(km)} \qquad (18a)$$

$$R_t = R_e + H_t \qquad \text{(km)} \qquad (18b)$$

where:

$$R_e = \text{average Earth radius} = 6\,371 \qquad \text{(km)} \qquad (18c)$$

Step 2: Calculate the Cartesian coordinates of the space station where the axes origin is at the centre of the Earth, the Z axis is directed northwards (such that the north pole is on the positive Z axis), and the X axis is in the meridian of the Earth-based station:

$$X_1 = R_s \cos(\varphi_s) \cos(\delta) \qquad \text{(km)} \qquad (19a)$$

$$Y_1 = R_s \cos(\varphi_s) \sin(\delta) \qquad \text{(km)} \qquad (19b)$$

$$Z_1 = R_s \sin(\varphi_s) \qquad \text{(km)} \qquad (19c)$$

Step 3: Rotate the Cartesian axes around the Y axis such that the Z axis passes through the Earth-based station, and then move the origin, without rotation, such that the origin coincides with the Earth-based station:

$$X_2 = X_1 \sin(\varphi_t) - Z_1 \cos(\varphi_t) \qquad \text{(km)} \qquad (20a)$$

$$Y_2 = Y_1 \qquad \text{(km)} \qquad (20b)$$

$$Z_2 = Z_1 \sin(\varphi_t) + X_1 \cos(\varphi_t) - R_t \qquad \text{(km)} \qquad (20c)$$

Step 4: Calculate the straight-line distance between the Earth-based station and the space station:

$$D_{ts} = \sqrt{X_2{}^2 + Y_2{}^2 + Z_2{}^2} \qquad \text{(km)} \qquad (21)$$

Step 5: Calculate the length of the line represented by D_{ts} projected into the X,Y plane:

$$G_{ts} = \sqrt{X_2{}^2 + Y_2{}^2} \qquad \text{(km)} \qquad (22)$$

Step 6: Calculate the elevation angle of the straight line from the Earth-based station to the space station:

$$\theta_0 = \text{atan2}(G_{ts}, Z_2) \qquad \text{(angle above horizontal)} \qquad (23)$$

where the function atan2(*x*, *y*) returns angle arctan(*x*/*y*) for any quadrant of a complete circle.

Step 7: Initially calculate the azimuthal bearing of the straight line from the Earth-based station to the space station relative to true South:

$$\psi = \text{atan2}(X_2, Y_2) \qquad (24)$$

Step 8: Reassign ψ to be eastwards from true North by subtracting it from a half-circle. Depending on the implementation of the atan2 function, the bearing may need to be processed into the range (0-360) degrees. The bearing is indeterminate if the elevation angle represents a vertical path.

Equation (23) gives the elevation angle of the ray at the Earth-based station θ_0 which would exist in the absence of tropospheric refraction, sometime referred to as the free-space elevation angle. The apparent elevation angle θ can be estimated from θ_0 using equation (25) in Attachment B.

Attachment B
to Annex 1

Conversion between apparent and free-space elevation angles

The following expressions provide conversion between two interpretations of the elevation angle of a space station as viewed from an Earth-based station:

i) *Free-space elevation angle* θ_0: the elevation angle calculated without taking atmospheric refraction into account.

ii) *Apparent or actual elevation*: the elevation angle calculated taking atmospheric refraction into account. This is optimum elevation angle for a high-gain antenna at the Earth-based station intended to provide a link to the space station.

Due to atmospheric refraction, θ is greater than the θ_0 under normal atmospheric conditions. The difference is greater at low elevation angles.

If θ_0 is known, θ is given by:

$$\theta = \theta_0 + \tau_{fs} \qquad \text{(degrees)} \qquad (25)$$

where θ_0 is in degrees, and τ_{fs} is the change in elevation angle due to refraction through the atmosphere. For an Earth-based station at altitude $H_t \leq 3$ km and for $-1 \leq \theta_0 \leq 10$ degrees, τ_{fs} may be estimated as:

$$\tau_{fs} = \frac{1}{T_{fs1} + H_t T_{fs2} + H_t^2 T_{fs3}} \qquad \text{(degrees)} \qquad (26)$$

where:

$$T_{fs1} = 1.728 + 0.5411\theta_0 + 0.037723\theta_0{}^2 \qquad (26a)$$

$$T_{fs2} = 0.1815 + 0.06272\,\theta_0 + 0.01380{\theta_0}^2 \qquad (26b)$$

$$T_{fs3} = 0.01727 + 0.0082888\theta_0 \qquad (26c)$$

If θ is known, θ_0 is given by:

$$\theta_0 = \theta - \tau \qquad \text{(degrees)} \qquad (27)$$

where τ can similarly be estimated as:

$$\tau = \frac{1}{T_1 + H_t T_2 + H_t^2 T_3} \qquad \text{(degrees)} \qquad (28)$$

where:

$$T_1 = 1.314 + 0.6437\theta + 0.02869\theta^2 \qquad (28a)$$

$$T_2 = 0.2305 + 0.09428\theta + 0.01096\,\theta^2 \qquad (28b)$$

$$T_3 = 0.008583 \qquad (28c)$$

Attachment C
to Annex 1

Attenuation due to atmospheric gasses

C.1   Introduction

This Attachment gives a procedure to evaluate attenuation due to atmospheric gasses for an Earth-space path, taking into account frequency, surface water-vapour density, station altitude, ground height, and the elevation angle at the Earth end of the path. Specific attenuation is calculated by reference to Recommendation ITU-R P.676 using the line-by-line method. The attenuation is summed over atmospheric layers using the general principle employed in Recommendation ITU-R P.676, with additional material from Recommendations ITU-R P.453 and ITU-R P.835, and extended to negative elevation angles, which can occur in certain situations, particularly in hilly terrain if the Earth-based station is situated well above sea-level.

It is valid for station altitudes up to 10 km above sea level, and up to 1 000 GHz.

The top level of the method is described in § C.2. Sub-sections C.3 to C.6 describe elements of the method which are invoked as required from earlier sections of this Attachment. Sections C.2 to C.5 are each described as step-by-step procedures, with the steps numbered from 1 in each case.

C.2   Attenuation due to atmospheric gaseous on an Earth-space path

The inputs to the calculation are:

H_t: altitude of Earth-based station (km above sea level)

H_g: terrain height at the Earth-based station (km above sea level)

θ: apparent ray elevation angle at the Earth-based station (degrees)

ρ_0:   surface water-vapour density (g/m^3)

f: frequency (GHz).

Step-by-step method

Step 1: Initialise an accumulator for attenuation:

$$A_{acc} = 0 \qquad \text{(dB)} \qquad (29)$$

Step 2: Initialise the ray altitude:

$$h = H_t \qquad \text{(km above sea level)} \qquad (30)$$

Step 3: Initialise the angle of the ray relative to vertical:

$$\beta = (90 - |\theta|)\frac{\pi}{180} \qquad \text{(radians)} \qquad (31)$$

The angle is formulated here in radians. It is used only in trigonometric functions, and should thus be in the appropriate units for the implementation in use. For this reason, subsequent references to the angle do not include units.

Step 4: Calculate the water-vapour density referred to sea level:

$$\rho_s = \rho_0 \exp\left(\frac{H_g}{2}\right) \qquad \text{(g/m}^3\text{)} \qquad (32)$$

Step 5: If $\theta < 0$, use the method in § C.3 below with the current values of h, β, ρ_s, f and A_{acc} as inputs, otherwise continue to Step 6. Note that equation (31) above gives a positive value for β even when θ is negative.

The calculation in § C.3 may assign new values to h, β and A_{acc}.

Step 6: Use the method in § C.4 below with the current values of h, β, ρ_s, f and A_{acc} as inputs. The calculation in § C.4 assigns a new value to A_{acc}.

Step 7: Assign attenuation due to atmospheric gasses:

$$A_g = A_{acc} \qquad \text{(dB)} \qquad (33)$$

C.3   Descending ray when traced from Earth-based station

This calculation is used only when called from Step 5 of § C.2 above. The inputs are the current values at the time of the call for the following:

    h : ray altitude, (km) above sea level

    β : ray angle relative to the local vertical

    ρ_s : water-vapour density referred to sea level (g/m^3)

    f : frequency (GHz)

   A_{acc} : accumulated attenuation (dB).

Step 1: Use the method in § C.5 below, with inputs h, ρ_s and f, to assign the following:

    t : temperature (K)

    p : dry-air pressure (hPa)

    e : water-vapour partial pressure (hPa)

    n : refractive index

    γ : specific gaseous attenuation (dB/km).

Step 2: Calculate the vertical thickness of the atmospheric layer:

$$\delta = 0.0001 + 0.01\max(h, 0) \qquad \text{(km)} \qquad (34)$$

Step 3: Initialise the radius of the lower edge of the atmospheric layer:

$$r = R_e + h - \delta \qquad \text{(km)} \qquad (35)$$

where R_e is true Earth radius = 6 371 km.

START OF LOOP FOR SUCCESSIVE ATMOSPHERIC LAYERS

Step 4: To test whether this is the atmospheric layer in which the elevation angle becomes positive, calculate the clearance, m (km), by which the current straight-line segment of the ray will pass over the lower boundary of the layer:

$$m = (r + \delta)\sin(\beta) - r \qquad \text{(km)} \qquad (36)$$

Step 5: If $m \geq 0$ the ray has reached a zero elevation angle within the current atmospheric layer, in which case do the following:

i)   calculate the horizontal path length, d (km), within the layer:

$$d_h = 2\sqrt{2r(\delta - m) + \delta^2 - m^2} \qquad \text{(km)} \qquad (37)$$

ii)   accumulate the attenuation:

$$A_{acc} = A_{acc} + d_h\gamma \qquad \text{(dB)} \qquad (38)$$

iii)   finish the calculation for the descending ray and continue from Step 6 of § C.2 with the current values to h, β and A_{acc}: Note that, if $m \geq 0$ occurs for the first atmospheric layer for a descending ray, the value of β will not have changed. Since Nevertheless, it will have the correct value when the calculation returns to Step 6 of § C.2.

Otherwise, $m < 0$ and the ray passes into the next atmospheric layer below, in which case continue here with Step 6.

Step 6: Calculate the slope distance through the atmospheric layer:

$$d_s = (r + \delta)\cos(\beta) - \sqrt{(r + \delta)^2\cos^2(\beta) - (2r\delta + \delta^2)} \qquad \text{(km)} \qquad (39)$$

Step 7: Accumulate attenuation:

$$A_{acc} = A_{acc} + d_s\gamma \qquad \text{(dB)} \qquad (40)$$

Step 8: Calculate the angle to the vertical at the lower edge of the current atmospheric layer:

$$\alpha = \arcsin\left[\frac{r+\delta}{r}\sin(\beta)\right] \qquad (41)$$

Step 9: Re-assign altitude for the next atmospheric layer:

$$h = h - \delta \qquad \text{(km above sea level)} \qquad (42)$$

Step 10: Re-assign the radius of the lower edge of the atmospheric layer:

$$r = r - \delta \qquad \text{(km)} \qquad (43)$$

Step 11: Use the method in § C.5 below, with inputs h, ρ_s and f, to re-assign t, p, e, and γ, but not to change the current value of refractive index n. Assign the new value of refractive index to a new variable n_{new}.

Step 12: Re-assign the vertical thickness of the atmospheric layer:

$$\delta = 0.0001 + 0.01\max(h, 0) \qquad \text{(km)} \qquad (44)$$

Step 13: Re-assign the ray angle relative to vertical at the upper edge of the atmospheric layer:

$$\beta = \arcsin\left[\frac{n}{n_{new}}\sin(\alpha)\right] \qquad (45)$$

Step 14: Re-assign the refractive index:

$$n = n_{new} \tag{46}$$

Step 15: Continue from Step 4 until the calculation ends in Step 5.

END OF LOOP

C.4   Ascending ray when traced from Earth-based station

This calculation is used only when called from Step 6 of § C.2 above. The inputs are the current values at the time of the call for the following:

> h : ray altitude, (km above sea level)
>
> β : ray angle relative to the local vertical
>
> ρ_s : water-vapour density referred to sea level (g/m^3)
>
> f : frequency (GHz)
>
> A_{acc} : accumulated attenuation (dB).

Step 1: Use the method in § C.5 below, with inputs h, ρ_s and f, to assign the following:

> t : temperature (K)
>
> p : dry-air pressure (hPa)
>
> e : water-vapour partial pressure (hPa)
>
> n : refractive index
>
> γ : specific gaseous attenuation (dB/km).

Step 2: Calculate the vertical thickness of the atmospheric layer:

$$\delta = 0.0001 + 0.01\max(h, 0) \qquad \text{(km)} \tag{47}$$

Step 3: Initialise the radius of the lower edge of the atmospheric layer:

$$r = R_e + h \qquad \text{(km)} \tag{48}$$

where R_e is true Earth radius = 6 371 km.

START OF LOOP FOR SUCCESSIVE ATMOSPHERIC LAYERS

Step 4: Calculate the slope distance through the atmospheric layer:

$$d_s = \sqrt{r^2\cos^2(\beta) + 2r\delta + \delta^2} - r\cos(\beta) \qquad \text{(km)} \tag{49}$$

Step 5: Accumulate attenuation:

$$A_{acc} = A_{acc} + d_s\gamma \qquad \text{(dB)} \tag{50}$$

Step 6: Re-assign the angle to the vertical at the upper edge of the current atmospheric layer:

$$\alpha = \arcsin\left[\frac{r}{r+\delta}\sin(\beta)\right] \tag{51}$$

Step 7: Re-assign altitude for the next atmospheric layer:

$$h = h + \delta \qquad \text{(km above sea level)} \tag{52}$$

Step 8: If $h \geq 100$, return to Step 7 of § C.2 above. Otherwise continue with Step 9.

Step 9: Re-assign the radius of the lower edge of the atmospheric layer:

$$r = r + \delta \qquad \text{(km)} \tag{53}$$

Step 10: Use the method in § C.5 below with inputs h, ρ_s and f, to re-assign t, p, e, and γ, but not to change the current value of refractive index n. Assign the new value of refractive index to a new variable, n_{new}.

Step 11: Re-assign the ray angle relative to vertical at the upper edge of the atmospheric layer:

$$\beta = \arcsin\left[\frac{n}{n_{new}}\sin(\alpha)\right] \tag{54}$$

Step 12: Re-assign the refractive index:

$$n = n_{new} \tag{55}$$

Step 13: Continue from Step 4 until the calculation ends in Step 8:

END OF LOOP

C.5 Atmospheric parameters

This procedure is used only when called from Step 11 of § C.3 or from Step 10 of § C.4, above. The inputs are the current values at the time of the call for the following:

> h: ray altitude, (km above sea level)
> ρ_s: water-vapour density referred to sea level (g/m³)
> f: frequency (GHz).

Step 1: Use the functions defined in § C.6 below to obtain temperature and dry-air partial pressure at height h as given by the reference atmosphere:

$$t = T_{ref}(h) \qquad (K) \tag{56a}$$

$$p = P_{ref}(h) \qquad (hPa) \tag{56b}$$

Step 2: Calculate water-vapour density at altitude h:

$$\rho = \rho_s \exp\left(\frac{-h}{2}\right) \qquad (g/m^3) \tag{57}$$

Step 3: Calculate water-vapour partial pressure at altitude h:

$$e = \frac{\rho t}{216.7} \qquad (hPa) \tag{58}$$

Step 4: Calculate refractive index n at altitude h:

$$n = 1 + 10^{-6}\left[\frac{77.6}{t}\left(p + e + 4810\frac{e}{t}\right)\right] \tag{59}$$

Step 5: Use the line-by-line method given in Recommendation ITU-R P.676 to calculate the specific attenuation due to gaseous absorption, γ (dB/km).

C.6 Reference atmosphere

The functions defined here are based on the United States Standard Atmosphere, 1976, as given in Recommendation ITU-R P.835, to obtain temperature and pressure for a given height above sea level.

Table C.1 gives constants required in the calculation:

TABLE C.1

Constants for the reference dry atmosphere

Row index i	Height, H_i (km asl)	Temperature Gradient, L_i (degrees K/km)	Temperature, T_i (degrees K)	Pressure, P_i (hPa)
0	0	−6.5	288.15	1013.25
1	11	0.0	216.65	226.323
2	20	1.0	216.65	54.750
3	32	2.8	228.65	8.680
4	47	0.0	270.65	1.109
5	51	−2.8	270.65	0.669
6	71	−2.0	214.65	0.040

Define functions $T_{ref}(h)$ and $P_{ref}(h)$ returning temperature, T_{ref} (K), and dry-air partial pressure, P_{ref} (hPa), as follows.

Find the highest value of index i given in the first column of Table C.1 for which H_i as given in the second column satisfies the condition $H_i \leq h$. If $h < 0$, set the index i to zero.

Temperature at height h is then given by:

$$T_{ref}(h) = T_i + L_i(h - H_i) \qquad \text{(K)} \tag{60}$$

and dry-air partial pressure at height h is given by:

$$P_{ref}(h) = \begin{cases} P_i \left[\dfrac{T_i}{T_i + L_i(h - H_i)}\right]^{\frac{34.163}{L_i}} & \text{If } L_i \neq 0 \\ P_i \exp\left[\dfrac{-34.163(h - H_i)}{T_i}\right] & \text{Otherwise} \end{cases} \qquad \text{(hPa)} \tag{61}$$

where H_i, L_i, T_i, and P_i are taken from the corresponding rows in Table C.1 on the row given by index i.

Attachment D
to Annex 1

Tropospheric scintillation

D.1   Introduction

Tropospheric scintillation is due to turbulence, which tends to be greatest in the atmospheric layer associated with cloud formation, and has the most effect on refractive index in the lower atmosphere.

The calculation described in this Attachment applies to a single path between one transmitter and one receiver. The scintillation mechanism does not absorb energy from a radio wave but only re-distributes it in a process of focussing and de-focussing, causing a distribution of spatial and temporal fades and enhancements.

Scintillation intensity is reduced by spatial averaging at an antenna with a large effective aperture compared to the spatial variability. Similarly, for multiple signals arriving at a victim receiver with similar strengths, scintillation fades and enhancements will tend to cancel, and the mechanism can then be ignored.

The calculation gives the scintillation enhancement level (dB) exceeded for a given percentage of time over which N_{wet} is averaged. The model is based on measurements for $0.01\% \leq p \leq (100\text{-}0.01)\%$, but gives feasible results for $0.001\% \leq p \leq (100\text{-}0.001)\%$. The enhancement is negative for $p > 50\%$, indicating a scintillation fade.

D.2 Scintillation intensity

Use the method given in § 2.4.1 of Recommendation ITU-R P.618-12 to calculate the scintillation intensity σ. If necessary the effective aperture of the Earth-based antenna, can be estimated from its antenna gain in the direction of the path using:

$$D_{eff} = 0.3 \cdot 10^{0.05 G_a}/(\pi \cdot f) \qquad \text{(m)} \qquad (62)$$

D.3 Tropospheric scintillation short-term variability

For a given scintillation intensity, σ_{st} , the short-term signal-level variability received by an antenna can be expressed as the enhancement and fades exceeded for given percentage times. Separate empirical expressions give factors for enhancements and fades when expressed in dB, as follows.

The factor for enhancements exceeded for p percent time, where ≤ 50 , is given by:

$$a_{ste}(p) = 2.672 - 1.258 \log(p) - 0.0835[\log(p)]^2 - 0.0597[\log(p)]^3 \qquad (63a)$$

The factor for fades exceeded for $(q = 100 - p)$ percent time, where > 50 , is given by:

$$a_{stf}(q) = 3.0 - 1.71 \log(q) + 0.072[\log(q)]^2 - 0.061[\log(q)]^3 \qquad (63b)$$

Thus the tropospheric scintillation attenuation not exceeded for p percent time is given by:

$$A_{st}(p) = \begin{cases} -\sigma_{st} a_{ste}(p) & \text{if } p \leq 50 \\ \sigma_{st} a_{stf}(100 - p) & \text{otherwise} \end{cases} \qquad \text{(dB)} \qquad (64)$$

Attenuation $A_{st}(p)$ is less than zero for $p < 50$ indicating an enhancement in signal level.

Attachment E
to Annex 1

Beam clearance taking atmospheric refraction into account

E.1

This Attachment gives a method for tracing a ray launched from an Earth-based station, in order to test whether it encounters an obstruction. It can be used to compile a profile of ray height relative to sea level, which can then be compared with a terrain profile.

The inputs to the method are:

H_t: Altitude of Earth-based station (km above sea level)

θ: Apparent elevation angle at the Earth-based station, θ ≤ 5 degrees.

Attachment A gives a method for calculating the free-space elevation angle of the path, θ_0. Equation (25) in Attachment B can be used to obtain the apparent elevation angle θ. It is possible for θ_0 or θ to be negative. Depending on terrain, this does not necessarily mean that the path is obstructed. Use of this method requires access to detailed topographical data which may need to be purchased.

Attachment A also permits the azimuthal direction of the Earth-space path to be calculated, which may be necessary to obtain a profile of the terrain under the path.

The calculation of vertical clearance proceeds as follows:

Notionally, a ray is launched at elevation angle θ and traced taking the vertical gradient of refractive index as a function of height into account. Equations (69) to (72) are repeated, each iteration producing new values of horizontal distance over curved earth D_c (km) and height of the ray above sea level, H_r (km), until the ray has reached a sufficient height to be clear of possible obstructions. The method is valid for H_r up to 10 km above sea level.

Initialise:

$$H_r = H_t \qquad \text{Ray altitude (km above sea level)} \qquad (65)$$

$$D_c = 0 \qquad \text{Horizontal distance over curved Earth (km)} \qquad (66)$$

$$\varepsilon = \theta \qquad \text{Ray elevation angle above local horizontal (radians)} \qquad (67)$$

Set the increment in horizontal distance over curved Earth:

$$\delta_d = 1 \qquad \text{(km)} \qquad (68)$$

Repeat equations (69) to (72) inclusive to calculate successive values of D_c and H_r:

START OF LOOP

Calculate the increment in ray elevation angle:

$$\delta_\varepsilon = \delta_d \left[\frac{1}{R_e} - 4.28715 \cdot 10^{-5} \exp\left(-\frac{H_r}{7.348}\right) \right] \qquad \text{(radians)} \qquad (69)$$

where R_e = 6 371 km, the average Earth radius.

Re-assign the ray height:

$$H_r = H_r + \delta_d \varepsilon \qquad \text{(km)} \qquad (70)$$

Re-assign the ray elevation angle:

$$\varepsilon = \varepsilon + \delta_\varepsilon \qquad \text{(radians)} \qquad (71)$$

Re-assign the horizontal distance over curved Earth:

$$D_c = D_c + \delta_d \qquad \text{(km)} \qquad (72)$$

END OF LOOP

The above loop should be continued until the ray height exceeds any possible terrestrial obstruction up to a maximum of 10 km above sea level. It may be convenient to store successive values of D_c and H_r in a two-column array which can then be compared against a profile of terrain and optionally other obstructions (noting that these are normally compiled with heights in metres) in the azimuthal direction given by Step 8 in Attachment A.

For elevation angles greater than 5 degrees, atmospheric refraction can be ignored, and the height of the ray at distance d (km) from the Earth-based station can be taken as:

$$H_r = H_t + d\tan(\theta) + \frac{d^2}{2R_e} \qquad \text{(km)} \qquad (73)$$

Attachment F
to Annex 1

Test for whether precipitation-scatter calculation is necessary

This Attachment describes a simple test which estimates the power received due to rain scattering in a common volume between two cylindrical antenna beams for a rain rate of R_{rain} mm/hr (1-minute integration time). The divergence of a beam with distance from its antenna is ignored.

The calculation method is biased towards over-estimating the scattered received power by ignoring rain attenuation along the rain-scatter path, and assuming that no power is absorbed by rain drops.

Figure F.1 shows the geometry of two cylinders representing antenna beams, denoted 1 and 2, of radii r_1 and r_2 (m), with $r_1 \leq r_2$, lengths L_1 and L_2 (m), and volumes V_1 and V_2 (m³). The centre-lines of the two cylinders coincide at the centre of the diagram. The angle between the direction of propagation of the incoming power in one cylinder and the scattered power travelling towards the victim receiver is the scatter angle θ. The test is considered reliable for $10 \leq \theta \leq 90$ degrees.

No significance should be attached to the orientation of the cylinders in Fig. F.1 with respect to the vertical. Either may be the Earth-space beam. However, one of the approximations used in the calculation is to assume uniform rain attenuation in the common volume of the two cylinders. Rain is not spatially uniform and this could lead to an overestimation of the loss. This test should not be used if the horizontal extent of the common volume exceeds $6\,600R_{rain}^{-0.08}$ metres.

The radii r_1 and r_2 should be calculated from the -3 dB beam edges of the two antennas at the point where their bore-sights coincide.

The test estimates the unwanted rain-scattered power received by the victim receiver exceeded for a given percentage time p.

FIGURE F.1

Common-volume of two cylindrical beams
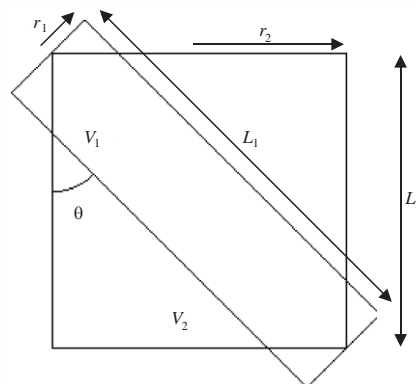
P.0619-F.1

The test is implemented by the following steps.

Step 1: Calculate the cylinder lengths:

$$L_1 = \frac{2r_2}{\sin(\theta)} \qquad \text{(m)} \tag{74a}$$

$$L_2 = \max(L_1 \cos(\theta), 2r_1 \sin(\theta)) \qquad \text{(m)} \tag{74b}$$

where the max function returns the larger of its two arguments.

Step 2: Calculate the power-flux density S in dB(W) incident upon the circular end of the cylinder representing the unwanted beam. This can be done in various ways. If the transmitter e.i.r.p. is available it given by:

$$S = P_{eirp} - 20\log(d_{tx}) - \gamma_g d_{tx} - 71.0 \qquad (\text{dB(W/m}^2)) \qquad (75)$$

where:

P_{eirp}: e.i.r.p. of the unwanted transmitter in dB(W)

d_{tx}: distance from the unwanted transmitter to the common volume in km

γ_g: specific attenuation due to atmospheric gasses in dB/km, as given by Recommendation ITU-R P.676.

P_{eirp} can be calculated as:

$$P_{eirp} = P_{tx} + G \qquad \text{dB(W)} \qquad (75a)$$

where:

P_{tx}: total radiated power of the unwanted transmitter in dB(W)

G: antenna gain in dBi in the direction of the common volume.

Step 3: Calculate the power entering the illuminated end of the cylinder representing the unwanted beam, according to whether this is cylinder 1 or 2.

If cylinder 1:

$$P_{in} = S + 10\log(\pi r_1{}^2) \qquad \text{dB(W)} \qquad (76a)$$

Otherwise:

$$P_{in} = S + 10\log(\pi r_2{}^2) \qquad \text{dB(W)} \qquad (76b)$$

Step 4: Calculate the power leaving the other end of the cylinder representing the unwanted beam, according to whether this is cylinder 1 or 2.

If cylinder 1:

$$P_{out} = P_{in} - 0.001\gamma_r L_1 \qquad \text{dB(W)} \qquad (77a)$$

Otherwise:

$$P_{out} = P_{in} - 0.001\gamma_r L_2 \qquad \text{dB(W)} \qquad (77b)$$

where:

γ_r is the specific rain attenuation rate exceeded for p% time given by:

$$\gamma_r = k R_{rain}{}^\alpha \qquad \text{dB/km} \qquad (77c)$$

R_{rain}: point rainfall rate in mm/h for a 1 minute integration time exceeded for *p*% time

k and α: regression coefficients given by Recommendation ITU-R P.838.

Step 5: Calculate the total power scattered from the cylinder representing the unwanted beam:

$$P_{scat} = 10\log(10^{0.1P_{in}} - 10^{0.1P_{out}}) \qquad \text{dB(W)} \qquad (78)$$

Step 6: Assuming, at this stage, that the rain scatter is isotropic, calculate the scattered e.i.r.p. within the common volume, according to whether the unwanted beam is represented by cylinder 1 or 2.

If cylinder 1:

$$P_{eirps} = P_{scat} \qquad \text{dB(W)} \qquad (79a)$$

Otherwise:

$$P_{eirps} = P_{scat} - 10 \log \left(\frac{r_2{}^2 L_2}{r_1{}^2 L_1} \right) \qquad \text{dB(W)} \qquad (79b)$$

Step 7: Calculate a factor to account for non-isotropic scattering above 10 GHz:

$$F_{nis} = \begin{matrix} 10^{-3} R_{rain}{}^{0.4} \cos(\theta) \{2(f - 10)^{1.6} - 2.5(f - 10)^{1.7}\} & \text{if } f > 10 \\ 0 & \text{otherwise} \end{matrix} \qquad \text{dB} \qquad (80)$$

where:

f: is the frequency in GHz.

Step 8: Estimate the unwanted scattered power received by the interfered-with antenna using:

$$P_{txs} = P_{eirps} + F_{nis} - 20\log(d_{rx}f) - \gamma_g d_{rx} - 92.4 \qquad \text{dB(W)} \qquad (81)$$

where:

d_{rx}: distance in km of the interfered-with antenna from the common volume represented by the cylinders

P_{txs}: an estimate of the unwanted scattered power. A full rain-scatter calculation should be conducted if $P_{int} - P_{txs} < 20$ dB, where P_{int} is the receiver's interference threshold.

_____